An investigation of the hardening process for several phosphate glass-containing cements

W. S. CHEN, E. A. MONROE, R. A. CONDRATE, SR, Y. M. GUO
NYS College of Ceramics, Alfred University, Alfred, NY 14802, USA

The hardening process for several phosphate glass-containing cements that have potential dental applications was investigated using both powder X-ray diffraction and Fourier-transform infrared spectral techniques. The investigated phosphate glasses contained various amounts of calcium, strontium and sodium ions. Crystalline brushite and amorphous phases whose concentrations and compositions depended on the compositions of the starting phases were formed during the hardening process for the cement. The study indicates that the use of phosphate glasses containing calcium and strontium ions in cement mixtures, rather than solid mixtures of the related metal oxides, sufficiently slows their hardening process so that commercially useful cements might be formed.

1. Introduction
Cold-setting reactions have been widely applied and studied for metal oxide–phosphoric acid cements [1]. Such cements are extremely useful for dental (or refractory) applications. Three types of reaction processes occur for these cements. The first type involves mixtures in which acidic or chemically inert oxides react very slightly or not at all with phosphoric acid. The second type involves mixtures in which highly basic oxides react violently with phosphoric acid so that a porous friable cement structure is generated. The third type involves mixtures in which phosphoric acid reacts with weakly basic or amphoteric oxides. This reaction process is rather slow and may not go to completion. This type of reacting mixture has generated commercially useful cements.

Finely powdered calcium and strontium oxides react dramatically with phosphoric acid, illustrating the second type of setting process. However, if calcium and strontium oxides are first calcined to form coarse particles, they may then react with phosphoric acid in a more controlled manner, generating a more commercially useful cement system.

Monroe and Chen investigated cements that involve the reaction of phosphate glass powders with phosphoric acid to form hardened products [2]. They found that better control of the hardening process for the resultant phosphate-containing cements can be obtained using such starting materials. Their investigated glass compositions contained oxides such as CaO, Na_2O and SrO. The present investigation was confined to obtaining information concerning the structural changes that occur during the hardening process that generates cements from such starting materials. Powder X-ray diffraction analyses and Fourier-transform infrared spectroscopy were used to characterize the structural nature of the starting

glass powders, and those of the crystalline and amorphous phases that were formed during hardening of the cement compositions investigated. Such structural information may lead to an understanding of how to optimize the formation and properties of the resultant hardened cement.

2. Experimental procedures
2.1. Glass preparation
Three different phosphate glass compositions containing calcium, strontium and/or sodium cations ($35CaO \cdot 35SrO \cdot 30P_2O_5$, $30CaO \cdot 30SrO \cdot 10Na_2O \cdot 30P_2O_5$ and $33.3CaO \cdot 33.3SrO \cdot 33.3P_2O_5$ for glasses A, B and C, respectively) were reacted with phosphoric acid to form hardened cement products. These phosphate glasses were prepared by conventional melting methods. Reagent grade sodium carbonate, strontium carbonate, calcium hydroxide and ammonium hydrogen phosphate [$(NH_4)_2HPO_4$] were mixed, ground and then calcined at 300 °C to eliminate NH_3. The calcined products were ground again, melted at 1320–1380 °C for 40 min in corundum crucibles and then quenched into water. The resultant glasses were dried at 105 °C for 4 h.

2.2. Cement preparation
The investigated glasses were powdered first using a mortar and pestle, then by a vibration mill for 2.5 h to yield powders with particle sizes < 10 μm. The liquid reactant for the setting reactions was aqueous 31.34 wt % H_3PO_4. The powder : liquid ratio for the setting reactions was determined by a standard cement wetting test to be 1.92 g ml^{-1}. The glass powder was first mixed with the liquid to form a paste consistency, and then placed in a humidity chamber at 37 °C for 2 h in

TABLE I Band locations (cm^{-1}) for glasses A, B and C along with related materials

Pyrophosphate materials [3]		Amorphous calcium Orthophosphate [PO$_4^{3-}$] [4]		Amorphous calcium pyro/orthophosphate [P$_2$O$_7^{4-}$/PO$_4^{3-}$] [4]	Glass		
Band range	Assignment	Wave number	Assignment		A	B	C
1210–1073	Asym. PO$_3$ stretch						
1076–1035	Sym. PO$_3$ stretch	1052	Asym. P–O stretch	1080 / 1045sh	1072	1061	1110	1073
1032–976	Asym PO$_3$ stretch						
980–937	Asym. P–O–P stretch	945sh	Sym. P–O stretch	930	930	935	935	936
758–722	Sym. P–O–P stretch			720	720	731	734	730
619–537	PO$_2$ bend	563	PO$_4$ bend	565	565	554	560	558

sh, Shoulder, sym., symmetrical, asym.. asymmetrical.

order to harden the cement. The setting times for these cements were < 10 min.

2.3. Characterization techniques

Powder X-ray diffraction patterns and infrared spectra were measured for powders of both the resultant hardened cements and the starting glass materials. The diffraction patterns were measured for the powders with a Philips Norelco diffractometer, using CuK_α radiation with a single-crystal graphite monochromator. Infrared absorption spectra were measured with a Nicolet 60-SXR Fourier-transform infrared interferometer using the KBr pellet technique.

3. Results and discussion
3.1. Characterization of the glasses

The powder X-ray diffraction patterns for the three glasses investigated are illustrated in Fig. 1. All of the diffraction patterns are very similar, possessing one broad amorphous peak at approximately 30° of 2θ. There are no sharp X-ray diffraction peaks indicating crystallinity for any of the glass samples. Therefore, infrared spectroscopy was a more useful tool for these glass samples to obtain structural information.

Fig. 2 shows the infrared spectra for the glass materials investigated, and Table I lists the band locations for each glass material compared with those reported in the literature for related phosphate phases [3, 4]. The observed band locations for the infrared bands of these glasses are close to those observed earlier for related pyrophosphate materials, except for the bands at 1061, 1110 and 1073 cm^{-1} for glasses A, B and C, respectively. Also, it may be noted from Fig. 2 that the band shoulders for glasses A and C at approximately 1000 cm^{-1} are more distinct and resolved than that for glass B.

The bands observed in the investigated infrared spectra are broad because glass phases possess non-periodic structures. Therefore, their vibrational bands are usually not as sharp as those observed for related crystalline phases. Many details in the infrared spectrum reported in the literature [4] for an amorphous mixture of calcium orthophosphate and pyrophosphate are very close to those observed for the currently investigated glasses, and this similarity presents strong evidence that the investigated glass structures contain both PO$_4^{3-}$ and P$_2$O$_7^{4-}$ ions. It is very difficult
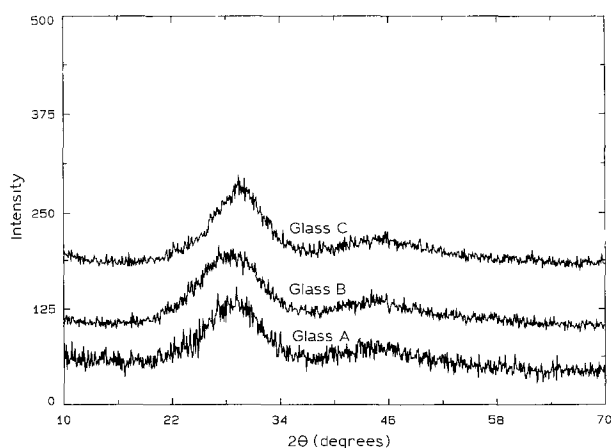

Figure 1 Powder X-ray diffraction patterns for the three glasses investigated which were used to obtain the hardened cements.
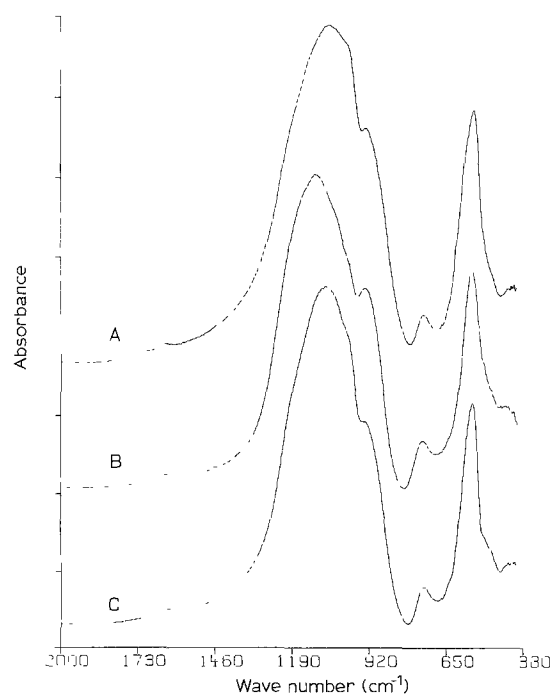

Figure 2 Infrared spectra for the three glasses investigated which were used to obtain hardened cements

to obtain structural information concerning the protonation of phosphate groups (particularly pyrophosphate groups) using the stretching and the bending modes of phosphate groups, because the observed infrared bands in this region are very broad and involve the convolution of bands from a number of different structural possibilities for these phosphate groups in the glass.

Corbridge [5] indicated that crystalline tribasic derivatives that contain orthophosphate ions possess a strong broad infrared absorption band between 1150 and 1000 cm^{-1}. Also, the infrared spectrum of amorphous calcium orthophosphate possesses a band at 1052 cm^{-1} (Table I). The observation that the infrared spectra for the present investigated glasses also possess a broad band between 1150 and 1000 cm^{-1} indicates that orthophosphate ions are probably present in these glasses. Corbridge [5] also suggested that a band between 750 and 650 cm^{-1} is characteristic of pyrophosphate ions, and can be assigned to a symmetric P–O–P stretching vibration for these ions. In the case of glasses A, B and C, infrared bands at approximately 730 cm^{-1} probably indicate the presence of pyrophosphate anions in their glass structures.

Corbridge and Lowe [6] assigned infrared bands in the 1170–1060, 1045–970, 940–870 and 735–690 cm^{-1} regions to pyrophosphate ions. However, the bands in the 1170–1060 and 1045–970 cm^{-1} regions overlap with infrared bands that occur for orthophosphate ions at approximately 1000 cm^{-1}. Therefore, the corresponding band in this region for the investigated glasses becomes very broad due to this overlap. This spectral condition creates the shoulder at approximately 1000 cm^{-1}. Because glasses A and C contained more modifier cations than glass B, their shoulders were more pronounced. The addition of modifier cations would promote the further formation of orthophosphate ions and would increase the intensity of the band observed at 1000 cm^{-1}.

The structural model for the investigated glasses predicted from the above spectral data is consistent with the theoretical model developed earlier for phosphate glasses [7]. The basic structural unit in a phosphate glass is the PO$_4$ tetrahedral unit. It can be attached to a maximum of three neighbouring PO$_4$ groups due to the P = O bond which must be present for each resultant structural unit when fully bond to other PO$_4$ groups. If modifiers such as CaO, SrO and Na$_2$O are added into the glass network, they break the P–O–P linkages and therefore create non-bridging oxygens. If the P$_2$O$_5$ content in a phosphate glass is 50 mol %, most of the PO$_4$ units are connected with less than three other PO$_4$ units. Its glass structure changes from a giant three-dimensional polymeric arrangement in which cross-linking is a maximum to chain structures in which only two rather than three of the bridging oxygens of a PO$_4$ tetrahedron can connect to other tetrahedra. For phosphate glasses containing $\leqslant$ 50 mol % P$_2$O$_5$ the average chain length can be predicted using the equation [7]

$$N = 2/\{[(m + 2m')/p] - 1\}$$

where N is the average number of tetrahedra in the chain, m is the molar fraction of monovalent cations, m' is the molar fraction of divalent cations and p is the molar fraction of phosphorus in the glass. Applying this theoretical model to glass B, where the P$_2$O$_5$ content is 33.3 mol % and the molar (CaO + SrO)/ P$_2$O$_5$ ratio is > 1 indicates that only a chain structure should exist in the glass network. The average chains for the phosphate groups in the glass involves only two tetrahedra, resulting in mainly pyrophosphate units.

Upon melting phosphate glasses, water may be incorporated into the glass network from either the raw materials or the atmosphere. The water also behaves as a glass modifier, reducing chain lengths by hydrolysing P–O–P linkages to produce chain-terminating P–O–H linkages. The infrared spectrum of glass B possesses two weak bands at approximately 3450 and 1623 cm^{-1}, due to water. Because of incorporated water, the average chain lengths in glass B would probably be less than two phosphate tetrahedra per chain, so that a significant number of orthophosphate ions should be found in addition to pyrophosphate ions.

In the case of the other two glasses investigated the molar (CaO + SrO)/P$_2$O$_5$ ratio for glass A and the molar (CaO + SrO + Na$_2$O)/P$_2$O$_5$ ratio for glass C were 2.3. Therefore, glasses A and C should not possess a polymeric cross-linking structure, but should possess chain structures similar to those in glass B. For these cases the average number of phosphate tetrahedra in a chain (N) is 1.4, indicating that these two glasses should contain more orthophosphate ions than glass B.

3.2. Characterization of the hardened cements

A back-scattered scanning electron microscopy (SEM) micrograph for the hardened cement formed from glass B is shown in Fig. 3. The microstructure of the hardened cement consisted of particles embedded in a matrix. This observation was true for the micrographs
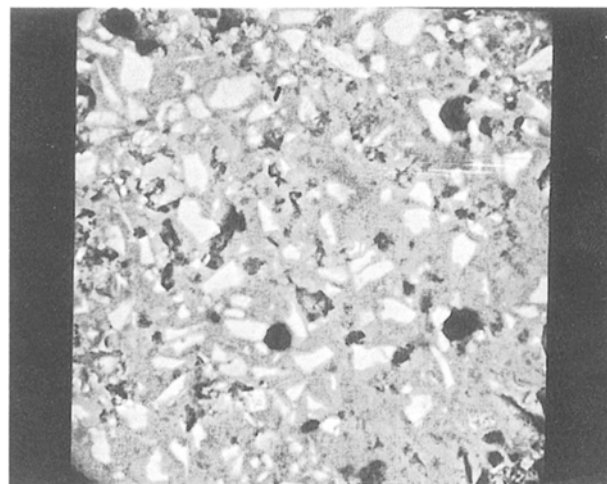

Figure 3 Back-scattered SEM micrograph for the hardened cement formed with glass B ($\times$ 700)

TABLE II Powder X-ray diffraction data for cement A and brushite

Brushite [8, 9]		Cement A (observed)	
d (nm)	I/I_0	d (nm)	I/I_0
0.757	100	0.768	67
0.424	100	0.428	100
0.305	75	0.307	68
0 2928	50	0 2941	46
0.2623	50	0.2666	16
0.2603	30		
0.2172	20	0.2157	17
0.2148	16		

TABLE III Related band locations (cm^{-1}) for cement A and brushite

Cement A	Brushite[8]	
	Wave number	Assignment
3482	3545	v_1 (H$_2$O stretch)
	3490	
	3280	v_3 (H$_2$O stretch)
	3160	
2930	2930	
	2380	v_1 (O$_3$PO–H stretch)
	2270	
	2140	
1647	1650	v_2 (H$_2$O bend)
	1215	v_5 (POH bend)
	1200	
	1140	v_6 (P–O stretch)
	1123	
1064	1075	
	1057	
	1000	v_2 (P–O stretch)
986	984	
874	875	v_3 (P–OH stretch)
793	785	
659	665	Water liberation
	663	
577	583	v_4 (O–P–O bend)
527	535	v_7 (O–P–O bend)
	519	

of all of the hardened cements investigated. The embedded particles involve unreacted glass powder residue whereas the matrix involves the reaction product from the hardening process, which is composed of the resultant crystalline and/or amorphous phase.

The powder X-ray diffraction patterns for hardened cements A, B and C are shown in Fig. 4. This figure, along with the X-ray diffraction data that are listed for cement A and brushite in Table II, clearly indicates that larger amounts of brushite (CaHPO$_4$ · 2H$_2$O) are present in cement A. Also, an amorphous peak may be noted at approximately 30° of 2θ, indicating remnants of unreacted glass and/or the new amorphous matrix product. The powder X-ray diffraction patterns in Fig. 4 for cements B and C indicate very small amounts of brushite in the resultant cements. Also, the X-ray broad diffraction peak at 30° of 2θ indicates an amorphous phase. These latter results are similar to those for cement A, except that less brushite is present. The shifts in the d-spacings of the crystalline brushite in the cement with respect to the literature values (Table II) probably indicates that the brushite crystals embedded in the cement matrix possess some stress from being enclosed in the cement matrix.

The infrared spectra for cements A, B and C, along with those of brushite, are shown in Fig. 5. The band assignments for the observed bands of cement A are listed in Table III. Comparing the infrared spectrum of brushite with that of cement A indicates that some bands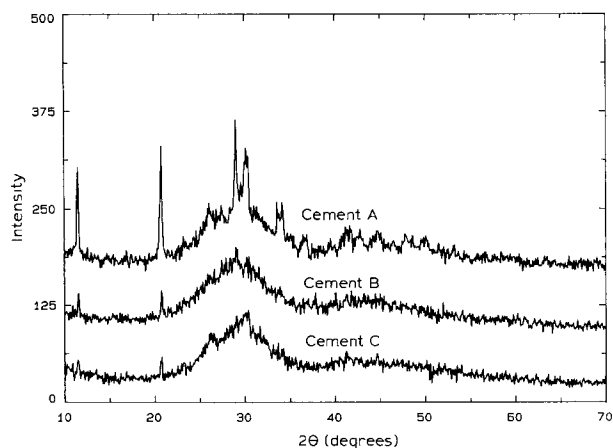 of brushite are not observed because they are masked by the broad bands of the glass. Table IV lists the band locations for cements B and C, together with those for related anhydrous pyrophosphates, two hydrated amorphous pyrophosphates and a hydrated crystalline pyrophosphate. The infrared bands noted
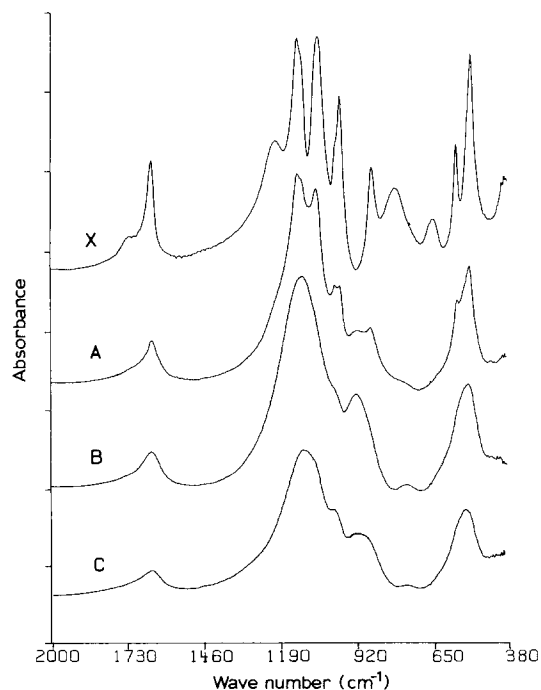

Figure 4 Powder X-ray diffraction patterns for the three hardened cements formed with the different glasses.

Figure 5 Infrared spectra for the three hardened cements formed with the different glasses and calcium brushite (X).

TABLE IV Band locations (cm^{-1}) for cements B and C and related pyrophosphates

Pyrophosphate materials [P$_2$O$_7^{4-}$] [3]		Ca$_2$P$_2$O$_7$ · 5H$_2$O [3]		Ca$_2$P$_2$O$_7$ · xH$_2$O (amorphous) [4]	Cement	
Band range	Assignment	Ordered	Disordered	Disordered	C	B
1210–1073	Asym. PO$_3$ stretch	1191vs 1150vs 1125vs 1092vs	1140vs	1124vs	1114s	1116s
1076–1035	Sym. PO$_3$ stretch	1040m	1042m	1032m		
1032–976	Asym. PO$_3$ stretch	1007m	1005w	990w	1007sh	1002sh
980–937	Asym. P–O–P stretch	958s 937s	926s	920s	935m	928m
758–722	Sym. P–O–P stretch	730w	730w	722w	748w	750w
619–537	PO$_2$ bend	600s 570s 547s	554s	560s	542s	536s

s, Strong; vs, very strong; m, medium, w, weak; sym., symmetrical; asym., asymmetrical

for cements B and C distinctly fall into the range noted for the infrared bands noted above for investigated pyrophosphates (Table IV). Also, the spectra of the cement are similar to those of disordered crystalline Ca$_2$P$_2$O$_7$·5H$_2$O as well as those of hydrated amorphous pyrophosphate cited earlier [4, 8, 9]. However, the band features or locations of the cement are not exactly the same as those of the disordered crystalline Ca$_2$P$_2$O$_7$·5H$_2$O.

Several factors may cause differences in the spectra with respect to the related phases. First, slight variations in the structures of the pyrophosphate ions (for example, variation either in the P–O bond distances or in the O–P–O or P–O–P bond angles) could cause the band positions to vary over a range of wave numbers. Secondly, orthophosphate ions should be present in the amorphous component of the matrix material, similarly to the investigated starting glass materials, and therefore their bands will convolute on to the resulting infrared spectra. Thirdly, varying amounts of water in hydrated phosphates could also influence their wave numbers. Either hydrogen bonding between water and phosphate groups or protonation of the phosphate groups could cause band shifts. Fourthly, cement B was made from glass that contained SrO and CaO, whereas cement C was made from glass that contained CaO, SrO and Na$_2$O. The nature of the cations around the anions can influence their band locations. Finally, the unreacted glass particles in the cement generate infrared bands that are superimposed on those of the reacted matrix. Therefore, the bands that we discussed for the final amorphous phase are really a convolution of the bands remaining for the unreacted glass, together with those also observed for the newly formed amorphous phase.

3.3. Nature of the cement hardening reaction mechanisms

In order to determine the nature of the cement hardening reaction mechanisms, it is first important to examine the types of reactions that can occur between glass and phosphoric acid solution during the hardening

process. These reactions can include acid–base, hydrolysis and hydration reactions [7].

During the acid–base reactions, Ca and Sr cations in the glass are exchanged by H ions in the glass, and are dissolved into acidic solution. The phosphate ions undergo hydration according to the process described earlier by Bunker et al. [7]. For glass A, the glass structure of which contains both pyrophosphate and orthophosphate groups, the latter groups may be easily released. Hydrolysis cleaves the P–O–P bonds of the pyrophosphate groups and leads to the formation of orthophosphate anions possessing OH bonds. The hydrolysis process exhibits a pH dependence, so in an acid solution the hydrolysis reaction is accelerated. For glass A, this reaction step could occur on the
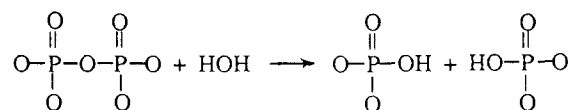
basis of the reaction. Therefore, due to these types of reactions, some Ca and Sr cations along with orthophosphate and hydrogen phosphate anions dissolve into the acidic solution. When the ion concentration product is greater than the pK of brushite, and the pH is low, brushite will be produced. This type of reaction did occur for all the glasses investigated.

Glasses B and C reacted with the added acid solution to generate mainly an amorphous hydrated pyrophosphate product. Such phase developments are expected on the basis of Corbridge [10], who noted that orthophosphoric acid often reacted with mixtures of metal oxides to form amorphous phases that were reluctant to crystallize. Glass C contained mixtures of calcium, strontium and sodium oxides. Its infrared spectrum indicated that a mixture of P$_2$O$_7$ and PO$_4$ groups were present in its glass network. This glass can dissolve into the acid solution and involve the three types of reaction that were mentioned above. The presence of a metal oxide mixture in this case is consistent with the conditions that Corbridge indicated to be necessary to form amorphous pyrophosphate products. The infrared spectrum of cement B indicates that it has similar structural features to

cement C. The atomic ratio of (Ca + Sr)/P for both glasses B and C was 1.0. Powder X-ray diffraction analysis indicated that cement A contained more brushite than either cement B or cement C, which contained mainly an amorphous phosphate phase. Therefore, the molar ratio of alkaline earths to phosphorus appeared to be critical in determining the amounts of brushite and the hydrated amorphous phosphate that were formed.

The formation of calcium and/or strontium brushite along with the resultant hydrated amorphous phosphate phase appear to be critical aspects associated with the mechanism for the setting or hardening of the investigated mixtures into a strong cement. Kingery [1] indicated that the hydrogen bonding of which the acid phosphates groups are capable provides on the surface of each crystallite of a material such as brushite the capability of extended chemical bonding with other related crystals in its vicinity as well as a strong internal structure. The hydrogen phosphate groups on these crystalline particles may also hydrogen bond with related groups on the surfaces of glass particles, forming strong bonds between them. Similar hydrogen bonds can be expected between glass particles if acid phosphate groups are also found on their surfaces. Finally, the hydrogen phosphates have a strong tendency to undergo various degrees of hydration, which consumes the water and therefore promotes the hardening process.

4. Conclusions

The hardening reaction rate is very important for forming a useful cement. Pure calcium and/or strontium oxide cannot react under normal conditions with phosphoric acid at a rate sufficient to generate useful cements, because their reaction rates are too rapid. On the other hand, cement precursor materials that include the investigated phosphate glass compositions containing such cations can react with phosphoric acid at a much slower rate that is more compatible for hardening processes to form useful cement products. In these cases the glasses must first be dissociated (a slow process) before the dissociated products can react to form either crystalline brushite or amorphous hydrated phosphates. The relative concentrations of these latter phases in the hardened product depends on the cation content in the initial glass composition before hardening. Finally, hydrogen bonding between the crystalline and glass-particle phases in the investigated cement materials apparently help to increase their strengths.

References

1   W D KINGERY, J Amer. Ceram. Soc. 33 (1950) 242.
2. E A MONROE and W S CHEN, Mater. Res. Soc Symp. Proc. 110 (1989) 611.
3. B C. CORNILSEN, PhD thesis, Alfred University, New York (1976).
4. J D TERMINE and D R LUNDY. Calcif. Tissue Res. 15 (1974) 55
5. D E C. CORBRIDGE, in "Topics in Phosphorus Chemistry", Vol. 6, edited by M. Grayson and E. J. Griffith (Interscience, New York, 1969) p. 235–65.
6. D E. C. CORBRIDGE and E J LOWE, J. Chem. Soc. (1954) 493.
7. B C BUNKER, G W ARNOLD and J. A. WILDER, J. Non-Cryst. Solids 64 (1984) 291
8. F CASCIANI and R A. CONDRATE, SR, Spectrosc. Lett. 12 (1979) 699.
9. F CASCIANI, PhD. thesis, Alfred University, New York (1978).
10. D E C CORBRIDGE, "Phosphorus Studies in Inorganic Chemistry", Vol. 6 (Elsevier, Amsterdam, 1985).